

Structure and variability of the Leeuwin Current in the south eastern Indian Ocean

Benny N. Peter, P.Sreeraj¹ and K.G.Vimal Kumar²

Research Institute for Applied Mechanics, Kyushu University, Kasuga, Fukuoka, 816-8580 Japan

¹Cochin University of Science & Technology

Dept. of Physical Oceanography, Cochin - 682 016

²National Institute of Oceanography, Regional Centre, Cochin

E.mail: benny@riam.kyushu-u.ac.jp, benny@gmail.com

ABSTRACT

The present study analyses the structure and variability of the Leeuwin Current in the south Indian Ocean. Besides the historic hydrographic dataset various observations made during WOCE, TOGA and other experiments conducted in the study region are employed. The long-term average bimonthly dynamic topography with reference to 400db is prepared to infer the spatial and temporal current pattern. In addition to the temperature-salinity profiles, the temperature profiles are also included in the estimation of dynamic height employing the correlation between heat content and dynamic height. Sections of hydrographic properties are also present at different latitudes of the Leeuwin Current region. Intra-annual variability of the Leeuwin Current is clearly illustrated in the bimonthly maps. The Leeuwin Current shows strong spatial and temporal variations. It is strong in southern winter and weak during summer. The current is broad and shallow in the north but becomes narrower and deeper in the south.

INTRODUCTION

Among the eastern boundary currents, the Leeuwin Current in the South Indian Ocean is unique in that it is poleward and flows against the prevailing wind. The Leeuwin Current is a warm ocean current that flows strongly southwards along the western Australian Coast, before turning eastwards at Cape Leeuwin and continuing into the Great Australian Bight where its influence extends as far as Tasmania.

The Leeuwin Current is quite different from the cool, northward flowing currents found along the southwest African coast (the Benguela Current) and the long Chile-Peru coast (the Humboldt Current), where upwelling of cool nutrient-rich waters from below the surface results in some of the most productive fisheries.

Because of the Leeuwin Current, the continental shelf water of western Australia is warmer in winter than the corresponding regions off southern Africa and Chile in summer. The Leeuwin Current is also responsible for the presence of true corals at the Abrolhos Islands and the transport of tropical marine species down the west coast and across into the Great Australian Bight. The Leeuwin Current is also known to be influenced by El-Niño conditions, with slightly

lower sea levels along the western Australian Coast and a weaker Leeuwin Current.

In view of the significance of the Leeuwin Current in physical & biological aspects of the Indian Ocean, efforts were made to understand the structure and variability of the Leeuwin Current by working out the bimonthly dynamic topography as well as the water characteristics and geostrophic flow pattern in the present study.

Earlier studies

Earliest documentation of the characteristics of Leeuwin Current were Saville - Kent (1897), Dakin (1919), Rochford (1969), Colborn (1975), Markma (1976). Cresswell & Golding (1980) used satellite tracked drifting buoys whereas, Legeckis & Cresswell (1981) Pearce & Cresswell (1985) analysed the satellite images and confirmed the earlier concepts of the southward transport of warm water of the Leeuwin Current.

Later, the Leeuwin Current Interdisciplinary Experiment (LUCIE), a field experiment co-ordinated by Australian CSIRO division of Oceanography during 1986-87 to understand the Leeuwin Current. The results of the experiment were accounted by Church,

Cresswell & Godfrey (1989), Smith et al. (1991) and Cresswell (1991).

Different theories were proposed (Thompson 1984, Cane (1983), Nicholls (1984), Godfrey & Weaver, (1990), Weaver & Middleton (1990) to explain the formation of Leeuwin Current.

Modelling studies of Leeuwin Current were carried out by Godfrey & Ridgeway (1985), Kundu & McCreary (1986), McCreary, Shetye & Kundu (1986) Thompson (1987), Weaver & Middleton (1989), Batteen & Butler (1998). Recent studies of Morrow et al. (2003), Feng et al. (2003) accounts the eddy circulation and the Elnino effects on Leeuwin Current.

DATA AND METHOD

In addition to the historic hydrographic data set, various observations made during World Ocean's Circulation Experiment(WOCE), Tropical Ocean Global Atmosphere (TOGA) and other experiments conducted in the eastern Indian Ocean region between 5°S-35°S and 100°E-120°E were made use of in the present study. The locations of hydrographic stations used for preparing the vertical sections are given in Fig (1) and the details in Table 1.

Table: 1 Details of hydrographic section used

ONE TIME		
Section	Ship	Date
I03	R/V KNORR	04.25.95-05.02.95
I05E	R/V KNORR	04.08.95-04.14.95
I05P	R/V CHARLES DARWIN	12.09.87-12.16.87
I10	R/V KNORR	11.13.95-11.19.95
REPEAT		
Section	Ship	Date
IR06A	FRANKLIN	04.02.95-04.22.95
IR06B	FRANKLIN	09.14.95-09.22.95

Vertical Sections of temperature and salinity up to 500m along various latitudes off Western Australia are prepared to understand the water characteristics of Leeuwin Current region. The long-term average bimonthly dynamic topography with reference to 400db has been estimated and presented to infer the circulation pattern of the study region.

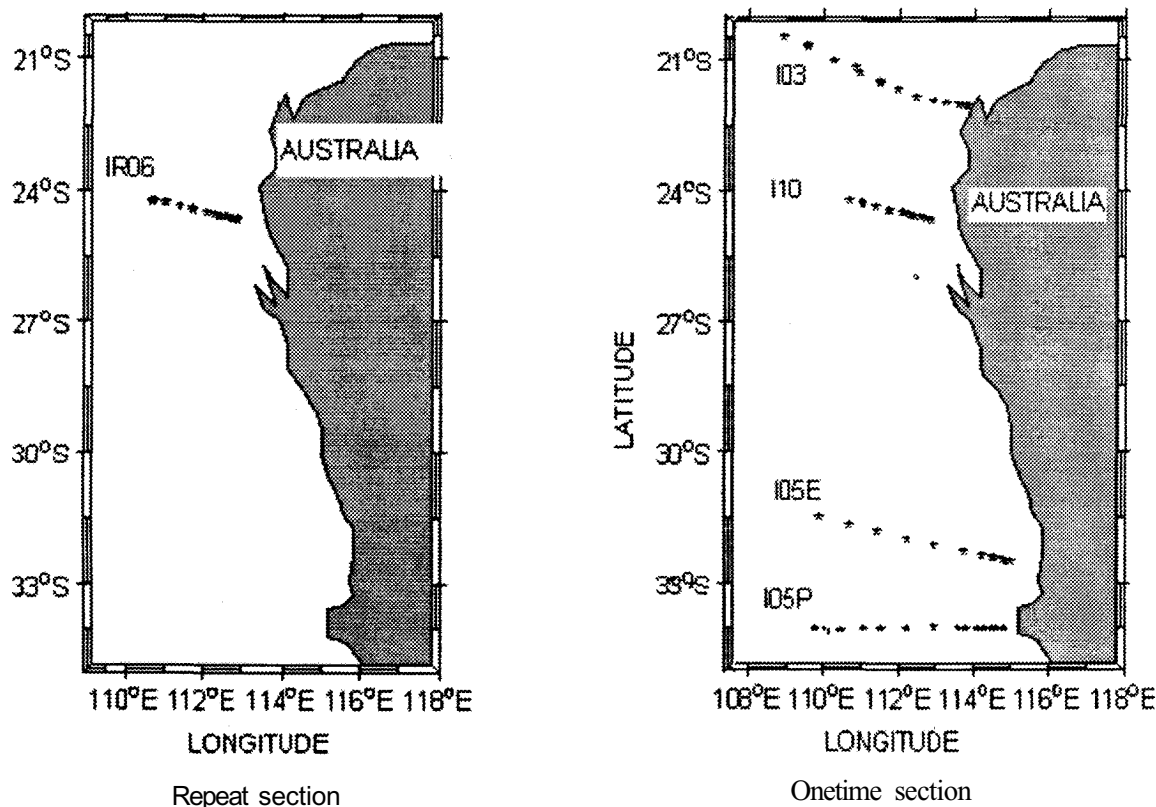


Figure 1. Location of hydrographic sections used

The anomaly of the dynamic depth (ΔD) is given by

$$\Delta D = \int_0^p \delta \, dp$$

where δ is the specific volume anomaly and 'p' is the pressure in decibars.

Geostrophic velocity across the repeat sections has been estimated and vertical sections are presented to understand the current flow. The geostrophic velocity between two stations along different sections are computed using the Helland - Hansen equation,

$$v = (10 / fL) (\Delta D_A - \Delta D_B)$$

where v = average current velocity normal to a line between stations A and B, $D_A - D_B$ = Dynamic height difference between stations A and B, L = distance between stations A and B, f = Coriolis parameter

For preparing the long-term average bimonthly dynamic topography the major handicap is the lack of necessary observations. Employing the existing temperature/salinity profiles alone, it is not possible to give an adequate description of annual cycle of dynamic topography. Therefore, in the present study we included the temperature/depth profiles also to estimate the dynamic height employing the correlation between heat content and dynamic height (Benny & Mizuno, 2000). Thus, including the temperature/depth observations (Fig.2), the long-term average bimonthly dynamic topographic maps were prepared.

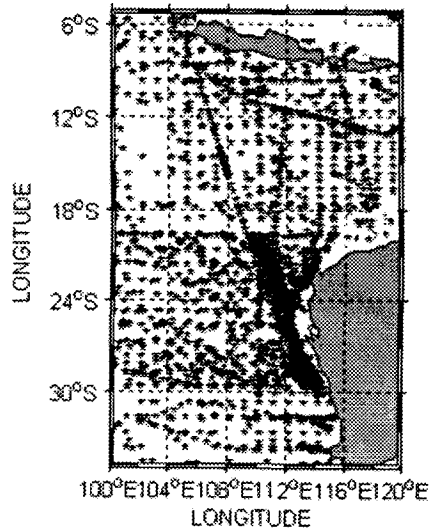


Figure 2. Stations used for estimating dynamic topography

RESULTS

Circulation

The long-term average bimonthly dynamic topography with reference to 400db has been prepared to understand the circulation pattern of the region.

The long-term mean dynamic topography of Jan-Feb shows zonal flow off Western Australia (Fig. 3). The Leeuwin Current is absent during the period. The Indonesian throughflow is mainly contributed by the flow through Lombok Strait. The flow off the Java coast is towards southeast. Eddy circulation is observed between 10°S and 20°S where the Indonesian throughflow merges with south equatorial current. Maximum steric height of 1.30 dynamic metres is observed in the throughflow region.

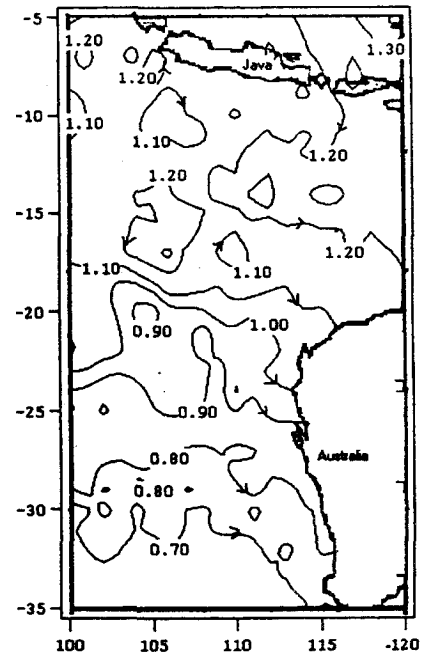


Figure 3. Dynamic topography January-February

Initiation of a southward flow is identified along the western coast off Australia during March-April (Fig.4). The flow direction is almost towards south in the northern part. The steric height is much increased in the Timor Strait region. Southeastward flow off Java is still present. The return flow of Indonesian throughflow is also strong during this period. Eddies are still present where the throughflow and the South Equatorial Current merge.

Dynamic topography during May-June (Fig.5) shows the presence of a strong southward flow along the coast off western Australia and the flow seems to turning eastward at Cape Leeuwin and continuing to the Great Australian Bight. The steric gradient shows strong flow between 112°E and 113°E. Another tremendous change observed in this period is the reversal of the flow off South Java that the flow is towards north westward. Eddies observed in the earlier periods are almost diffused. Indonesian throughflow is also weak during the period.

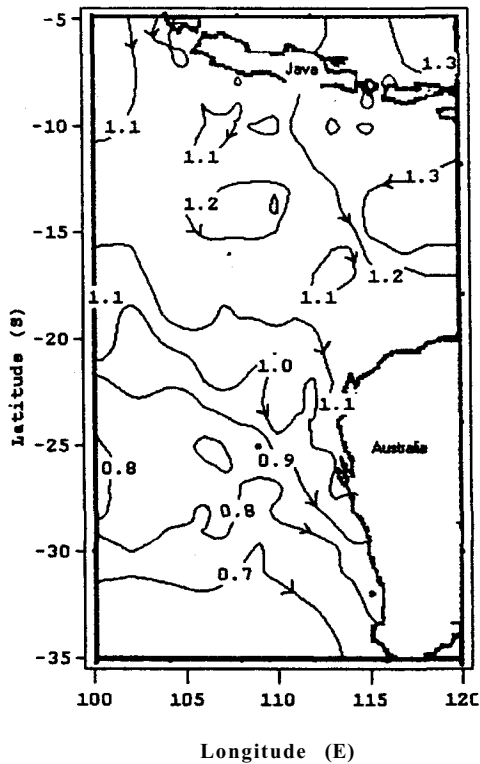


Figure 4. Dynamic topography March-April

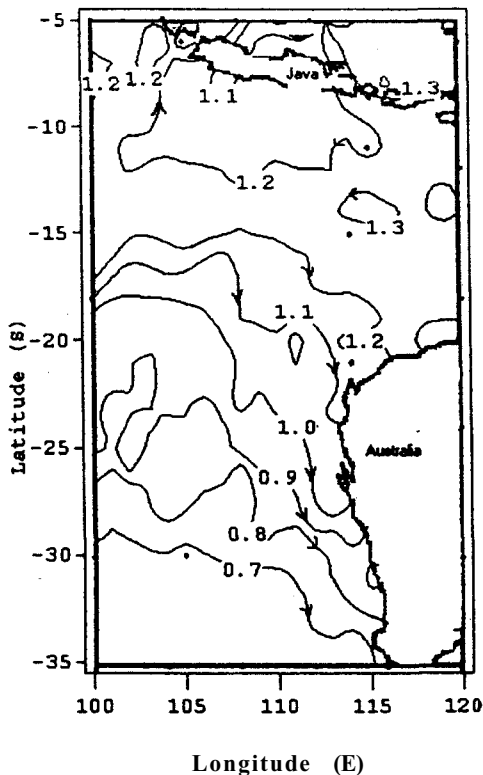


Figure 5. Dynamic topography May-June

It is interesting to note that even though the southward flow off western Australia in the north was already ceased, a strong southerly flow exists beyond 25°S between 110°E and 113°E during July-August (Fig.6). Instead of southward flow, a zonal flow is occurring in north-west part of Australia. Indonesian throughflow is very prominent during this period and it seems that the flows through Lombok Strait and Timor Strait are equally contributing. The flow along South Java coast is towards northwest and is embedded with cyclonic eddies during the period.

The dynamic topography (Fig.7) during September - October shows zonal flow between 20°S and 30°S off Western Australia. A southward flow still exists off Cape Leeuwin. Alternate northward and southward flow is observed between 105°E and 115°E and 20°S and 30°S. Indonesian throughflow is strong. The steric heights show a very strong cyclonic circulation off South Java. It is interesting to note that the northern part of the region is dynamically very active during this period. Very high steric height of 1.4 dynamic metres is observed between 10°S and 15°S in the western side.

The dynamic topography during November-December is shown in Fig.8. Steric height is reduced at 5°S - 15° S regions. The major contribution of the Indonesian throughflow is from the Lombok Strait. The cyclonic circulation off Java is also weakened. Off the Western Australia the flow pattern shows a northward flow between 20°S and 25°S during this period. In the south, zonal flow prevails. Weak circulation is observed in the central part.

Water Characteristics

Vertical Sections of temperature and salinity along various latitudes off Western Australia arc prepared to understand the water characteristics of Leeuwin Current region.

I03

The vertical salinity distribution shows strong horizontal variations in surface layers up to 50m (Fig.9a). High salinity is observed in the eastern part of the section, and a strong variation is noticed at around 111°E in the surface layers. A tongue like intrusion of high salinity water is identified between 100 m and 300 m from west up to 112°E. A halocline is present between 250 m and 400 m where a variation of 0.7 psu is observed

The vertical section of temperature between 107° E and 114°E covered during April - May along the section I03 displays in Fig. 9(b). The distribution shows slightly warm surface water in the west near

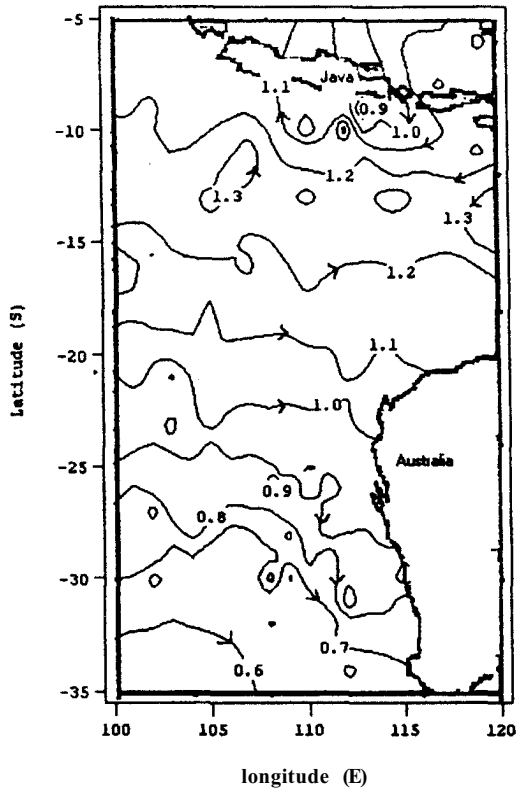


Figure 6. Dynamic topography July-August

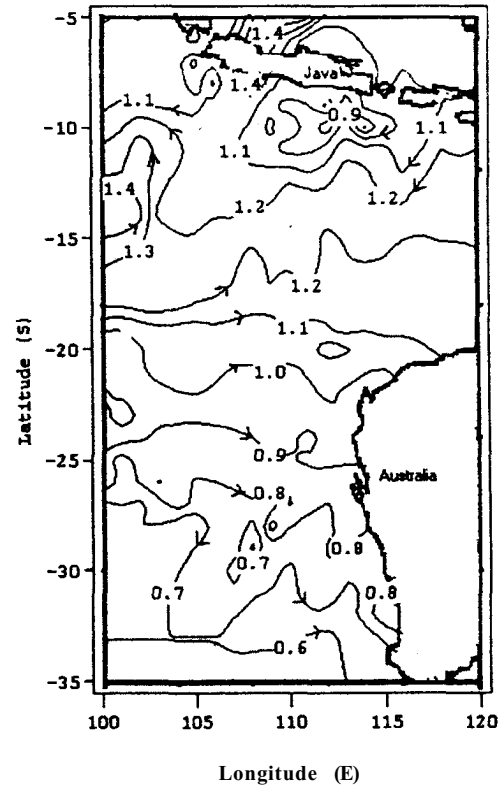


Figure 7. Dynamic topography September-October

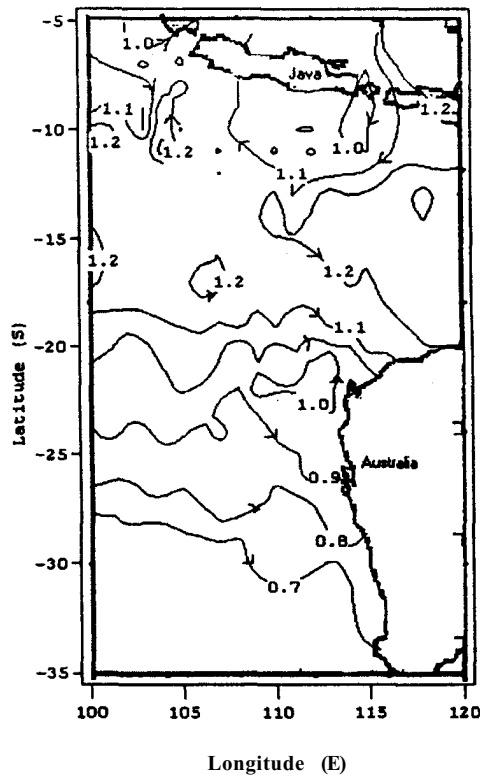


Figure 8. Dynamic topography November-December

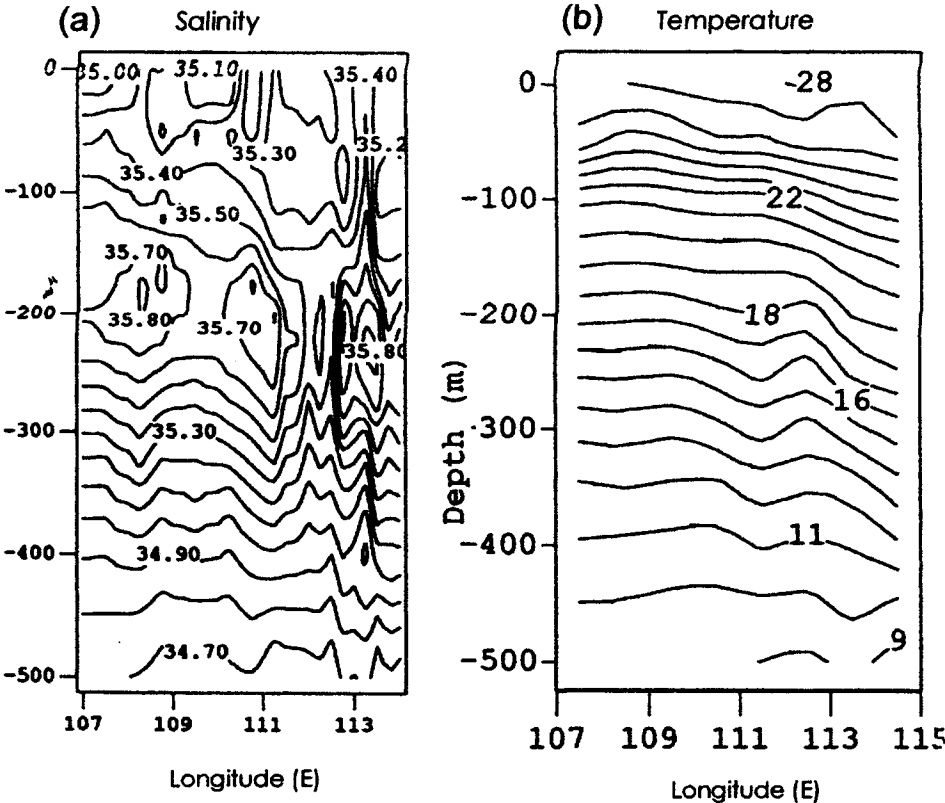


Figure 9 (a) & (b) Vertical section of salinity and temperature along I03

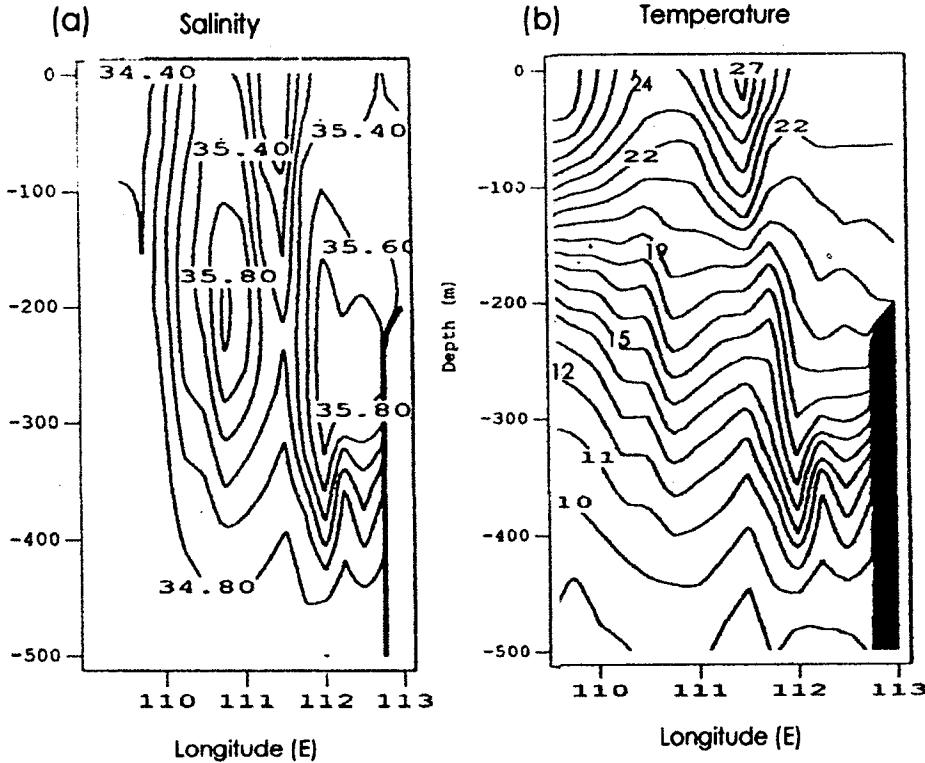


Figure 10 (a) & (b) Vertical section of salinity and temperature along I10

to Australia. The isotherms are sloping downward towards east up to a depth of 400 m and they are almost horizontal below. The mixed layer is very thin and a very shallow thermocline from 25 m to about 300 m is observed, where the decrease in temperature is about 15°C.

I05E

The vertical section of salinity corresponding to I05E shows a well-defined isohaline layer up to 80 m between 110°E and 113°E (Fig.10a). Beyond 113° E, horizontal variation is prominent at the surface. A strong halocline is present between 80 m and 300 m in the western part. It is interesting to note that the halocline shows a downward sloping towards east from 113°E as in temperature distribution. In addition, between 50 m and 200 m depths, salinity is almost constant in the eastern part.

The vertical temperature distribution between 110°E and 115°E during April is shown in Fig. 10(b). The isotherms are sloping downwards towards east between 113°E and 115°E. Mixed layer is very thin and the horizontal variation is prominent in the eastern

part. A shallow thermocline is observed between 25m and 150m where a decrease of 8°C is identified.

I05P

In contrast to the earlier section (I05E) a well-defined isohaline layer is present in the eastern part which extends up to 80 m whereas, this layer is very shallow in the western part (Fig. 1 la). Almost constant salinity of about 35.80 psu is noticed at the surface from east to west. A halocline is present between 80 m and 300 m and the salinity gradient is stronger in the eastern part. The distribution shows a step like structure in the western part of the halocline whereas a crest like pattern is observed between 114°E and 115°E.

This section between 110°E and 115°E covered during December and shows very low surface temperatures are observed (Fig. 11b). An east-west temperature gradient of about 2°C is identified at the surface layers. The mixed is much deeper in the east compared to the earlier sections. The isotherms show a step like structure from west to east and are sloping towards east as in the earlier sections. A crest like formation is observed between 114°E and 115°E.

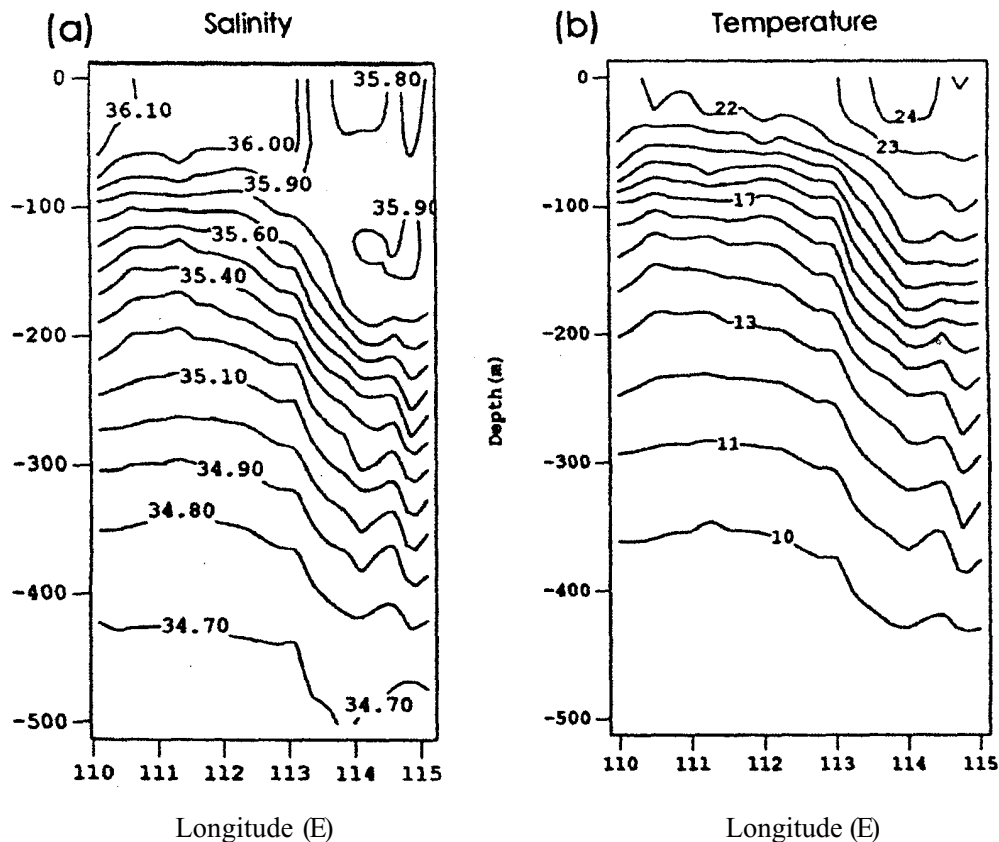


Figure 11 (a) & (b) Vertical section of salinity and temperature along I05E

A weak thermocline is present between 50 m and 400 m.

I10

Vertical salinity distribution along I10 also shows a very different pattern (Fig. 12a). Strong horizontal variation exists in the eastern part from 110°E to 111°E, whereas, almost homogeneous low salinity water is observed in the west. A strong salinity front exists around 110°E where a strong horizontal salinity variation of 1psu is found. In the eastern part between 100m and 400m the salinity structure shows two high salinity cells separated by low salinity

The vertical temperature distribution between 107°E and 113°E covered during November shows a very peculiar pattern (Fig. 12b). Horizontal variation is dominant between 109°E and 112°E from surface to 500 m. The surfacing of isotherms at 111°E illustrates the upwelling of cool subsurface waters, where a surface temperature of around 23°C is observed. Warm waters of temperature above 28°C are observed in the west whereas very cool waters of about 22°C are noticed in the east between 112°E and 113°E. A strong thermocline is identified between 50 m and 200 m in the west and it slopes downwards towards

east. The temperature gradient is very strong between 300 m and 400 m in the eastern end.

IR06A

Salinity distribution along the section (Fig. 13a) shows strong horizontal variations from east to west up to 200 m, while vertical variation is prominent between 200 m and 400 m. At the surface, the salinity varies from 34.4 psu to 35.6 psu (112°E). The variation is even strong between 108°E and 110°E. A homogeneous salinity layer of 35.2 psu is present from 112°E to 114°E up to 200 m. A weak halocline exists between 200 m and 400 m where the salinity varies from 35.6 psu to 34.8 psu. A high salinity cell of 35.8 psu is identified at the central part between 100 m and 300 m.

The section covered during April between 107°E and 114°E shows a well-mixed layer from west to east present between 0 and 50 m (Fig. 13b). Below the mixed layer a thermocline exists from 50 m to 300m. It is interesting to note that the thermocline is much stronger in the west and east compared to the central region having a gradient of 16°C exists. The isotherms exhibit a convex structure up to 100m and then show a concave structure below up to 500 m.

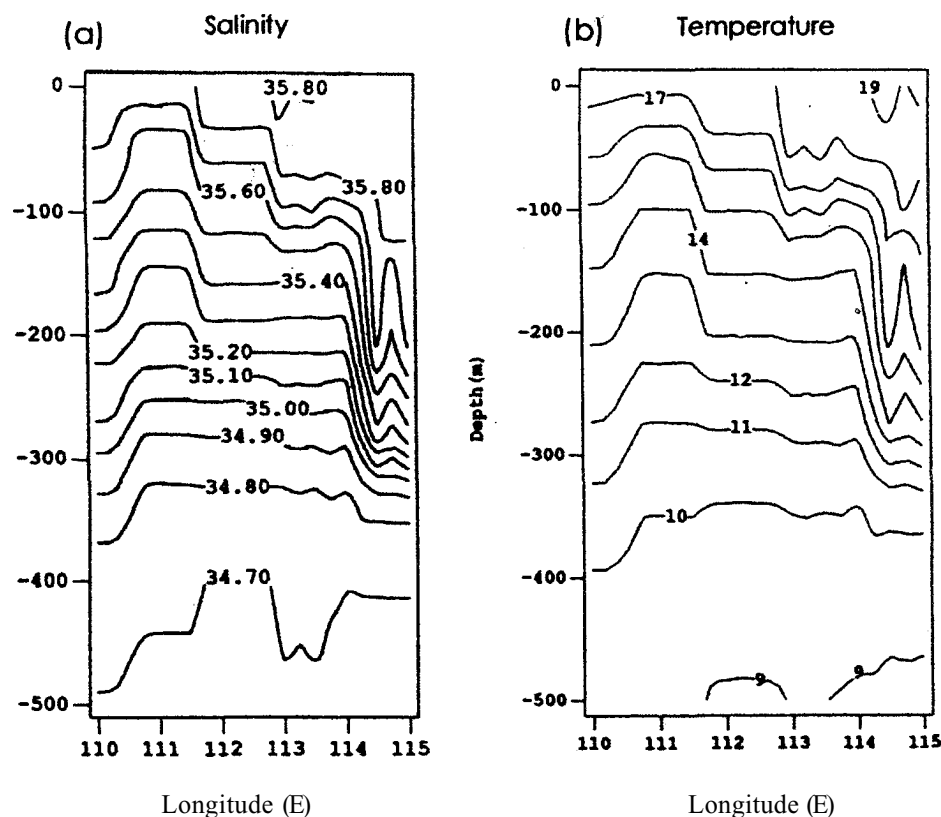


Figure 12 (a) & (b) Vertical section of salinity and temperature along I05P

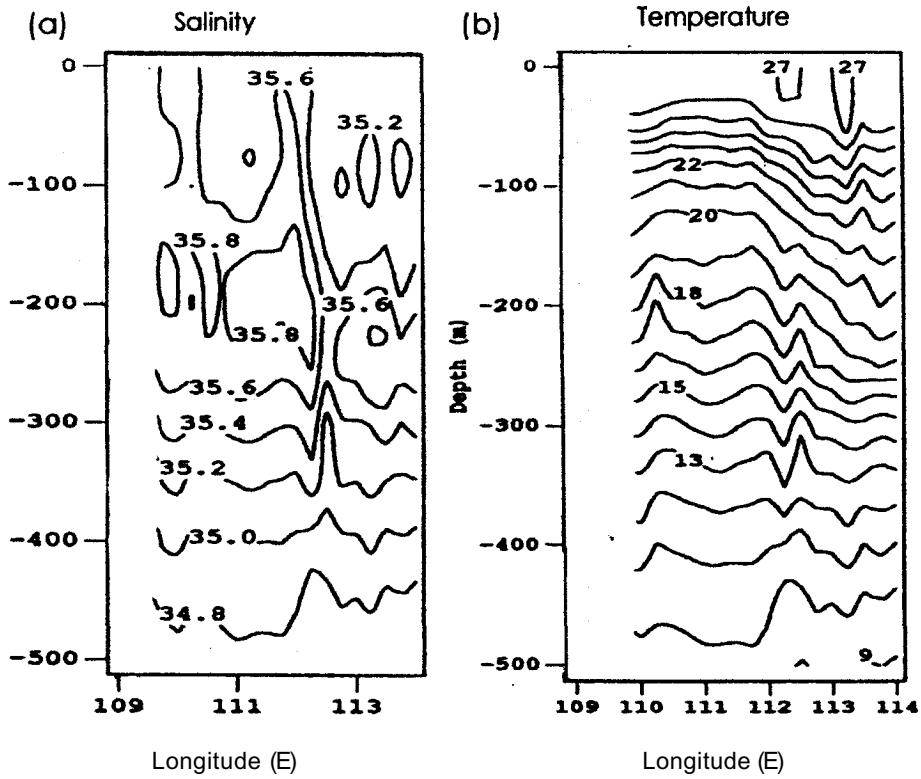


Figure 13 (a) & (b) Vertical section of salinity and temperature along IR06A

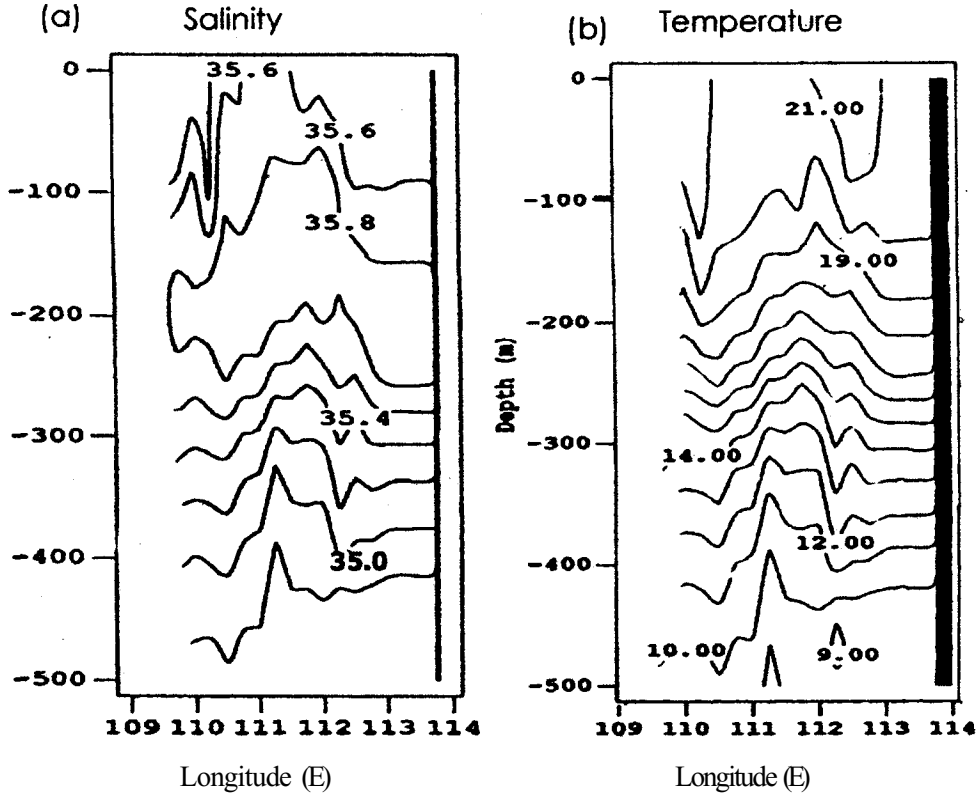


Figure 14 (a) & (b) Vertical section of salinity and temperature along IR06B

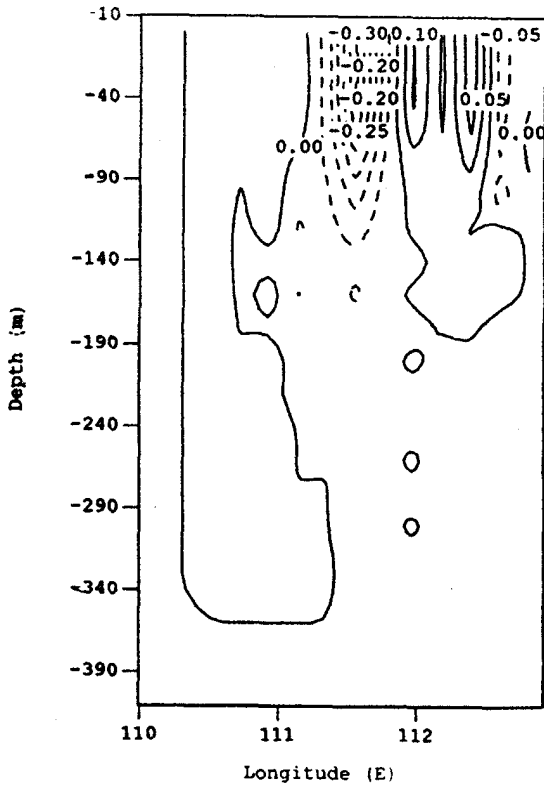


Figure 15. Geostrophic velocity-IR06A

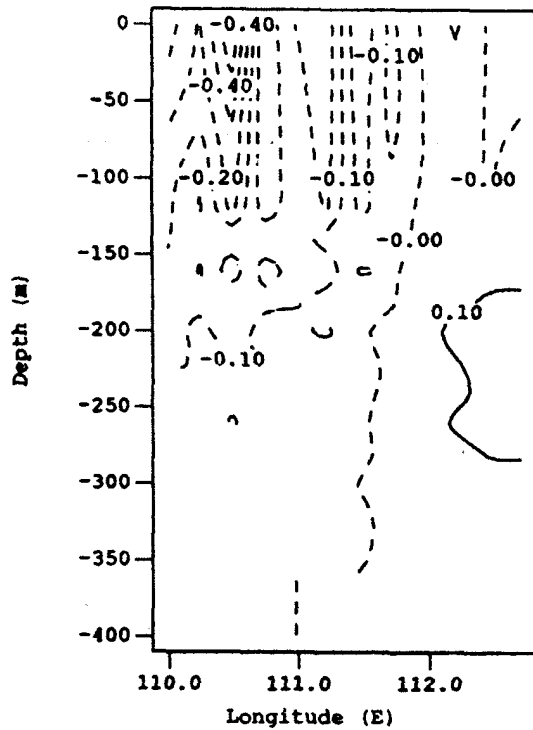


Figure 16. Geostrophic velocity-IR06B

IR06B

The vertical salinity distribution along IR06B (Fig. 14a) shows almost similar pattern that of IR06A except in the eastern part where high salinity water is present at the surface. A tongue like structure of high salinity extending from the east up to 108°E between 100 m and 300 m is identified. Halocline is very weak during this period.

The vertical distribution of temperature between 107°E and 114°E covered during September shows low surface temperature Fig. 14(b). A strong horizontal gradient of about 4°C is present up to 100 m from west to east. The mixed layer is deep and extends up to 100m along the section. Almost homogeneous water is observed up to 100m in the east. But a deep isothermal layer is present between 110°E and 112°E, from surface to a depth of 100 m. A weak thermocline is present from 100 m to 400 m where a decrease in temperature of 10°C is noticed. The isotherms exhibit wave like pattern in the thermocline region.

Geostrophic Velocity

The vertical section of geostrophic velocity with reference to 400db (Fig. 15) along IR06A section illustrates the strong southward flow of the Leeuwin Current around 112°E. The current is more broad and thin. Below 100 m, the flow is very weak. Towards west alternate northward and southward flows prevail

Tremendous changes occurred in the velocity structure of IR06B section compared to the earlier one (Fig. 16). The strong southward flow of the Leeuwin Current observed at around 112°E is not present. Instead, in the eastern part northward surface current is present

DISCUSSION

The annual cycle of the Leeuwin Current is clearly illustrated in long-term bimonthly dynamic topographic maps. The water characteristics and the geostrophic flow confirm the variability of the Lecuwin Current.

The dynamic topography maps exhibits the initiation of the Leeuwin Current during March-April. The flow around Northwest Cape turns towards south. But the southward flow is limited to 25 degree south and beyond south eastward flow exists. The vertical distribution of salinity and temperature also supports the development of southward flow of warm, low saline water (section IR06A). This agrees with the warm low saline signature of the Leeuwin Current

reported by Kitani (1977), Cresswell & Golding (1980). The geostrophic flow along the section IR06A clearly illustrates the southerly flow around 112°E. The flow is comparatively strong but shallow.

By May - June the Poleward flow is well developed along whole the coast off Western Australia and the current core is almost located between 112°E and 113°E. The warm low saline water observed in the region also confirms the presence of Leeuwin Current. Steric height is high in the Indonesian throughflow region.

During July - August, the Poleward flow is displaced by a zonal flow in the northwestern part of Australia whereas a strong southward flow of Leeuwin Current is still exists between 25°S and 35°S. It is interesting to note that a drastic decrease in steric height is occurring in the northern part especially in the Java Coast where a northwestward coastal current is present.

The Leeuwin Current is almost disappeared during September - October and a zonal flow is occurring. The presence of eddies confirm the change over of southward flow to zonal flow. The section IR06B also supports weakening of the Leeuwin Current. Instead of warm, low saline water the characteristics shows low temperature, high saline water. The steric heights are much lowered near Java and strong northward flow is observed there. It seems that as the throughflow and South Java Current get strengthened, the Leeuwin Current is weakened. Kundu & Mc Creary (1986) identified throughflow as a secondary forcing mechanism of Leeuwin Current.

During November - December instead of a southward flow, a reverse flow is occurring at northwest of Australia between 20°S and 25°S. It seems that southeast trades drive this flow and the thermohaline effects are negligible. The temperature - salinity structure also support the absence of strong southward flow of Leeuwin Current. Further the water characteristics along 110 are well agree with the long-term dynamic topography during November - December. The temperature section clearly exhibits a strong upwelling region at about 110°E and 112°E where the northward flow coupled with the northward wind results in upwelling. Salinity distribution also supports this feature. The Indonesian throughflow has weakened and steric height was slightly increased. Cresswell et al. (1989) and Pearce & Pattiaratchi (1999) also noticed a northward Capes current on the continental shelf during austral summer.

The northward flow observed between 20°S and 25°S is diffused during January - February and almost a weak zonal exists. Indonesian throughflow is

weakened and it is interesting to note that the South Java Current has reversed.

The seasonal as well as the spatial structure of Leeuwin Current is clearly established. The observations of Cresswell & Golding (1980), Pearce & Cresswell (1985) suggest that it is strongest during southern autumn and winter (months of April to August) and appears to weaken by about November. Feng et al., (2003) found that seasonally, the Leeuwin Current has the maximum geostrophic transport of 5 Sv during June - July at 32°S.

Model results (McCreary, Shetye & Kundu 1986; Kundu & McCreary, 1986 and Smith et al. 1991) suggest that the annual cycle is mostly due to the variations in the northward windstress, which is stronger during austral summer. Godfrey & Ridgeway (1985) and Morrow & Birol (1998) proposes that the annual variations of the meridional pressure gradients at shelf break may also contribute to the annual cycle of the Leeuwin Current

The dynamic topography shows that Leeuwin Current is broad and shallow in the north but narrow and deeper in the south. This is in agreement with the observations of Church, Cresswell & Godfrey (1989).

It is also interesting to note the slight longitudinal shift of Leeuwin Current especially in the southern part. During the time of strong flow the current is located between 112° E and 113° E, while in the weaker period it is around 114° E.

CONCLUSIONS

The long-term average bimonthly dynamic topography combined with thermohaline structure and geostrophic velocity estimations describe the structure and variability of the Leeuwin Current - the poleward eastern boundary current in the south Indian Ocean. The initiation, growth and decay of the current are clearly illustrated in the maps.

1. The Leeuwin Current is initiated in the northwest off Australia in March-April.

2. The Current is further strengthened and extends along whole the west coast of Australia by May - June.

3. By July - August the Current is weakened in the north. The southward flow is limited between 25° S - 35° S and the flow is zonal in the northwest off Australia.

4. Zonal flow prevails throughout the coast of Western Australia in September - October period.

5. In November-December even a reverse flow (northward) and associated upwelling occurs in the central part (25° S - 30° S).

6. Again, the flow becomes zonal by January-February.

Leeuwin Current shows an inverse relationship with South Java Current (SJC). During southern summer, the SJC is very strong and flows towards southwest, whereas in southern winter it is weak and flows north-westward. But, the Leeuwin Current is strong in southern winter and weak during summer.

Thus, the Leeuwin Current shows strong spatial and temporal variations. The current is broad and shallow in the north but becomes narrower and deeper in the south. It also exhibits slight temporal longitudinal shift.

REFERENCES

- Batteen, M.L. & Buttler, C.L., (1998). Modelling studies of Leeuwin Current off western and southern Australia, *J. P.O.*, 28, 2199-2221
- Benny, N. P. & Mizuno K., 2000. Annual cycle of steric heights in the Indian Ocean estimated from the thermal field, *Deep-Sea Res.*, 47, 1351-1368
- Cane, M.A., 1983. Oceanographic events during El-Nino, *Science*, 222, 1189-1195.
- Church, J.A., Creswell, G.R. & Godfrey, J.S., 1989. The Leeuwin Current-Poleward flow along Eastern Ocean boundaries, (eds.) Neshyba, S., Mooers, C.N.K. & Smith, R.L., Springer - Verlag Lecture Notes.
- Colborn, J.G., 1975. The thermal structure of Indian Ocean. International Indian Ocean Expedition Monogr. No.2.
- Cresswell, G. R., Boland, F.M., Peterson, J.L. & Wells, G.S., 1989. Continental shelf currents near the Abrolhos Islands, Western Australia, *Aust. J. Mar. Freshwater Res.*, 40, 113-128.
- Cresswell, G.R. & Golding, J.J., 1980. Observations of a south-flowing current in the southeast Indian Ocean. *Deep Sea Research*, 27A, 449 -466.
- Cresswell, G. R. (1991). The Leeuwin Current-Observations and recent models: In Leeuwin Current: an influence on the coastal climate and marine life of Western Australia, (eds.) Pearce, A.F. & Walker, D.I., *J. Roy Soc. WA* 74: 1-4
- Dakin, W.J., 1919. The Percy Sladen Trust Expedition to the Abrolhos Islands (Indian Ocean). *Rep.1, J. Linnean Soci.* 34, 127 - 180.
- Feng, M., Gary Meyers, Alan Pearce and Susan Wijffels 2003. Annual and interannual variations of the Leeuwin current at 32°S. *J.Geophys. Res.*, 108 (C11), 3355.
- Godfrey, J.S. & Ridgway, K.R., 1985. The large-scale environment of the poleward flowing Leeuwin Current, Western Australia: longshore steric height gradients, wind stresses and geostrophic flow. *J. Phys. Oceanogr.*, 15, 481-495.
- Godfrey, J.S. & Weaver, A.J., 1990. Is the Leeuwin Current driven by Pacific heating and winds? *Progress in oceanography*, Pergamon, 27, 225-272.
- Kitani, K., 1977. The movement and physical characteristics of the waters off Western Australia in November 1975, *Bull. Far Seas Fish. Res. Lab (Shimizu)*, 15, 13-19.
- Kundu, P.K. & McCreary, J.P., 1986. On the dynamics of the throughflow from the Indian Ocean. *J. Phys. Oceanogr* 16, 2191- 2198.
- Legeckis, R. & Cresswell, G.R., 1981. Satellite observations of sea surface temperature fronts of the coast of western and southern Australia, *Deep-Sea Res.*, 38 Suppl. S247-S271
- Markina, N.P., 1976. Biogeographic regionalization of Australian waters of the Indian Ocean. *Oceanology*, 15, 602- 604.
- McCreary, J.P., Shetye, S.R. & Kundu, P.K., 1986. Thermohaline forcing of eastern boundary currents with application to the circulation off the west coast of Australia. *J. Mar. Res.*, 44, 71-92.
- Morrow, R., & Birol, R., 1998. Variability in the southeast Indian Ocean from altimetry: Forcing mechanisms for the Leeuwin Current. *J. Geophys. Res.*, 103, 18529-18544.
- Morrow, R., Fangxin Fang, Michele Fieux, & Robert Molcard, 2003. Anatomy of three warm-core Leeuwin Current eddies. *Deep Sea Res. II*, 50 (12/13), 2229-2243.
- Nicholls, N., 1984. The Southern Oscillation and Indonesian Sea Surface temperature. *Mon. Weather Rev*, 112,424-432
- Pearce, A.F. & Cresswell, G.R., 1985. Ocean circulation off western Australia and the Leeuwin Current. *CSIRO Inf. Sheet*, 16-3, 4 pp.
- Pearce, A. F. & Pattiaratchi, C.B., 1999. The Capes current: a summer counter current flowing past Cape Leeuwin and Cape Naturaliste, southwestern Australia *Cont, Shelf Res.*, 19, 401-420
- Rochford, D.J., 1969. Seasonal variations in Indian Ocean along 110°E. I. Hydrological structure of the upper 500m. 20, 1-50.
- Saville - Kent, W, 1897. *The Naturalist in Australia*. Chapman & Hall, London, 388 pp.
- Smith, R.L., Huyer, A., Godfrey, J.S. & Church,

- J.A.,(1991. The Leeuwin Current off western Australia, *J. Phys. Oceanogr.*, 21, 323 - 345
- Thompson, R.O.R.Y.,1984. Observations of the Leeuwin Current off Western Australia. *J. Phys. Oceanogr.*, 19, 623-628.
- Thompson, R.O.R.Y, 1987. Continental - Shelf - Scale model of the Leeuwin Current. *J. Mar. Res.*, 45, 813-827.
- Weaver, A.J. & Middleton, J.H.,1989. On the dynamics of the Leeuwin Current, *J. Phys. Oceanogr.*, 19, 626-648.
- Weaver, A.J. & Middleton, J.H., 1990. An analytic model of Leeuwin Current off Western Australia, *Cont. Shelf Res.*, 10, 105-122.

(Accepted 2005 February 2. Received 2005 January 25; in original form 2004 August 18)